C00-3496-63

ENERGY DISSIPATION, MASS DIFFUSION AND INTERACTION TIMES FOR HEAVY ION COLLISIONS*,†

J.R. Huizenga, W.U. Schröder**, J.R. Birkelund and W. Wilcke

Departments of Chemistry and Physics and
Nuclear Structure Research Laboratory***
University of Rochester, Rochester, New York 14627

ABSTRACT

Correlations of experimental observables with kinetic energy loss and fragment mass for damped heavy ion reactions are emphasized in this paper. Angular-momentum-dependent interaction times are deduced giving a time scale for the evaluation of nucleon diffusion coefficients. The energy dissipated per nucleon exchange in Kr- and Xe-induced reactions is shown to decrease with increasing kinetic energy loss. These results are compared with predictions of a one-body dissipation mechanism and microscopic transport theory for heavy ion collisions. The relative decrease of energy dissipation due to nucleon exchange with decreasing bombarding energy is a new experimental feature that is unaccounted for by the above theories.

I. INTRODUCTION

There has been a large number of experimental studies of damped reactions involving a range of targets and projectiles.[1] The characteristic experimental features of heavy ion collisions which define this new reaction mechanism are:

a. Binary Process -- The damped reaction mechanism produces two massive primary fragments in the exit channel. However, light particles may be emitted from the intermediate system or, after its breakup, from the target-like or projectile-like primary fragments.

b. Energy Loss -- Damping of the initial relative kinetic energy of the target and projectile nuclei resulting in a range of kinetic energies down to the Coulomb energies for charge centers of highly deformed fragments. The broad energy distribution observed in experiments is the most distinctive property of damped reactions.

c. Nucleon Exchange -- Nucleon diffusion occurs during the short time the two nuclei are in contact. For the heavier ion reactions, the fragment mass distributions are peaked in the vicinity of the projectile and target masses.

d. Angular Distributions -- The angular distributions for products with projectile-like masses have properties of a fast peripheral or direct reaction process. The heavy systems usually rotate less than 180 degrees. Substantial sideways-peaking is observed for a number of systems while a forward rising angular distribution is a characteristic feature of other systems.

DISCLAIMER

e. Angular Momentum Transfer -- The primary fragments resulting from a damped collision may have rather large intrinsic angular momenta.

f. Light Particles and γ-rays -- As stated in (a) light particles (e.g., p, n and α particles) may be emitted from the intermediate system or, after its breakup, from the target-like or projectile-like primary fragments. The emission of γ-rays is mainly confined to the final stages of the fragment de-excitation.

In spite of the large number of experimental studies[1] of heavy ion reactions which report one or more of the characteristic features of damped reactions summarized above, only a relatively small number of studies have been performed where correlations of experimental observables, such as kinetic energy loss and fragment mass, are deduced. Hence, these correlations will be emphasized here. Angular-momentum dependent interaction times are deduced from experimental angular distributions. The angular momentum ℓ is related to the experimental kinetic-energy loss assuming the energy loss to increase monotonically with decreasing ℓ, i.e., increasing overlap of the matter distributions of projectile and target. The progressive increase in the variance of the charge distribution as a function of increasing kinetic energy loss is a feature common to all very heavy ion reactions studied so far. A quantitative correlation between the measured variance of the charge distributions and the amount of kinetic energy loss is employed to calculate the kinetic energy loss associated with the exchange of a single nucleon. The energy dependence of this quantity is compared with different theoretical models. Assuming the above time scale, nucleon diffusion coefficients are deduced from experimental fragment charge distributions.

II. ANGULAR, ENERGY AND MASS DISTRIBUTIONS FROM DAMPED REACTIONS

For illustration of the properties of damped collisions, we choose the $^{209}Bi + ^{136}Xe$ reaction which has been studied extensively. Some of the relevant parameters are listed below.

$E_{lab} = 1130$ MeV

$E_{c.m.} = 684$ MeV $\approx 1.6 \times E_{Coul}$

$\lambda\!\!\!^{-} = 0.019$ fm; $\quad 2a = 9.4$ fm

$\eta = Z_1 Z_2 e^2/\hbar v = a/\lambda\!\!\!^{-} = 245$

$\theta_{1/4} = 54°$ (c.m.)

$R_{SA} = 15.2$ fm

$\sigma_R = 2.8$ b

$\ell_{max} = 484\hbar$

The angular distribution of all lighter projectile-like fragments[2] in the total kinetic energy window, $300 \leq TKE \leq 650$ MeV, is shown in Fig. 1. The angular distribution peaks at 50° (c.m.) and is relatively narrow in width. There is no orbiting for this reaction, a phenomenon well known for selected lighter ion reactions. The charge distribution of the lighter fragments[2] for the above energy window and the angular range $25 \leq \theta_{c.m.} \leq 75$ is shown in Fig. 2. The drop of the charge distribution beyond symmetry (Z = 70) is due to experimental detection limits. Some contributions to the cross section for the lightest Z fragments is due to sequential fission of the heavy damped fragment. The continual range of total kinetic energy damping for the very heavy ion reactions[3] is illustrated in Fig. 3 where the differential cross section in millibarns per MeV of total kinetic energy loss is plotted versus the total kinetic energy loss. Hence, in speaking of damped heavy ion collisions we refer to a wide range of events with energy losses from a few MeV to hundreds of MeV. The kinetic energy loss indicated by each arrow in Fig. 3 corresponds to a final kinetic energy equivalent to the Coulomb energy at the strong absorption radius R_{SA}.

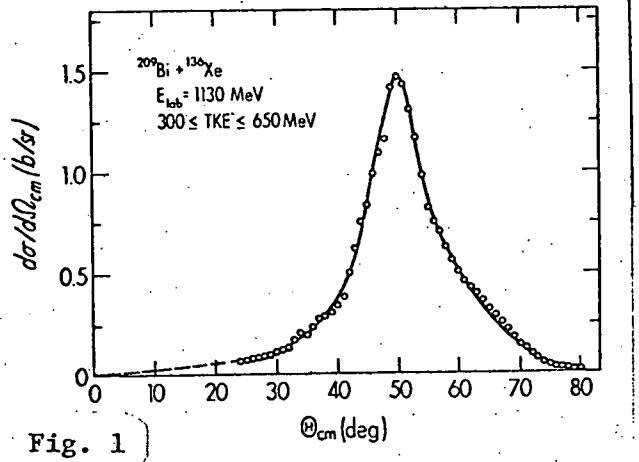

Fig. 1

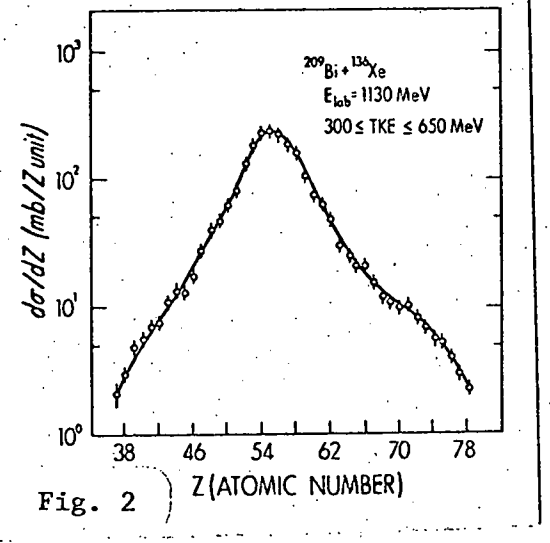

Fig. 2

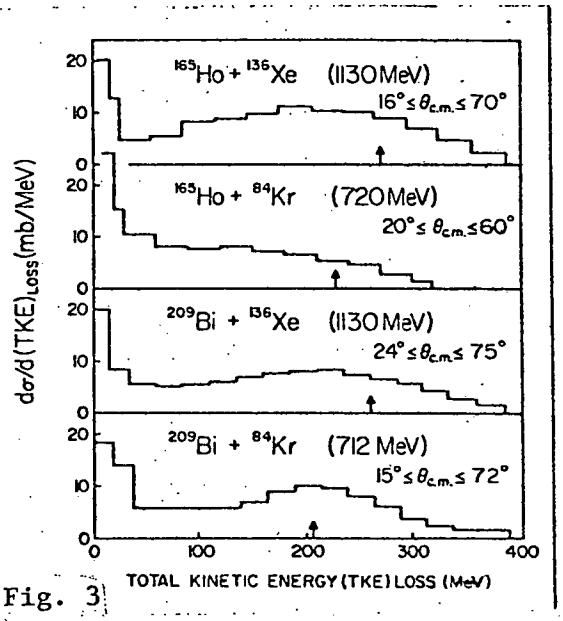

Fig. 3

III. CORRELATION OF EXPERIMENTAL OBSERVABLES IN DAMPED REACTIONS

A. Angular Distributions: Dependence on Mass Exchange and Energy Damping

The angular distributions for damped heavy ion collisions depend on mass (or charge) exchange and energy damping. In Fig. 4 is shown a contour plot of the double-differential cross section $d^2\sigma/d\Omega d(TKE)$ as a function of angle $\theta_{c.m.}$ for the $^{209}Bi + ^{136}Xe$ reaction.[2] Diagrams of this type were first drawn by Wilczyński.[4] For this reaction there is a cross section ridge that moves down in energy at an almost constant angle leading to what is known as strong angular focusing. Depending on the bombarding energy and parameters of the system, the cross section ridge in an energy-angle contour plot may move forward, stay constant or move backward in angle. For some of the lighter systems, an additional ridge at low energies moving backward in angle is observed. This is commonly interpreted as the reflection of the low-energy ridge at negative angles (orbiting).

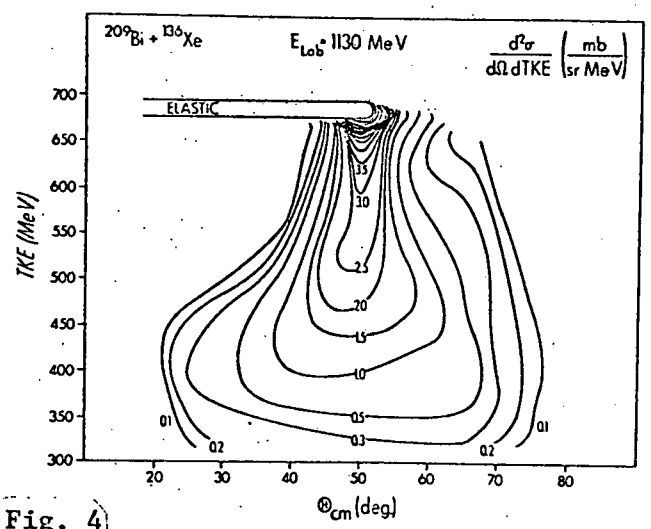

Fig. 4

The angular distributions for fixed TKE bins (50 MeV wide) are shown[2] in Fig. 5. Again one sees that the angular distributions are sideways-peaked for small energy losses and rather flat for large energy losses, although the maximum stays essentially constant at 50° c.m.. The angular distributions for fixed Z bins (3 Z units wide) are displayed in Fig. 6. For fragments near the projectile, the angular distributions are sideways-peaked and become less peaked for fragments far from the projectile. However, it is important to note that the angular distributions for fragments near the projectile change markedly with energy damping in much the same way as illustrated in Fig. 5 for all fragments. This is illustrated in Fig. 7 for Z = 53-55 and energy bins of 50 MeV width.[2] The observed dependence of the angular distribution on the fragment Z is only an apparent correlation which is due to the fact that the energy spectra corresponding to various fragments are somewhat different, as will be discussed below. Hence, the energy loss is a fundamental observable specifying the properties of the reaction. This is also shown in Fig. 8 where the full width at half maximum (FWHM) in the charge distribution is plotted as a

function of $\theta_{c.m.}$ for different final total kinetic energies.[2] Although the FWHM varies considerably for different TKE values, the value of the FWHM for a particular TKE is independent of angle.

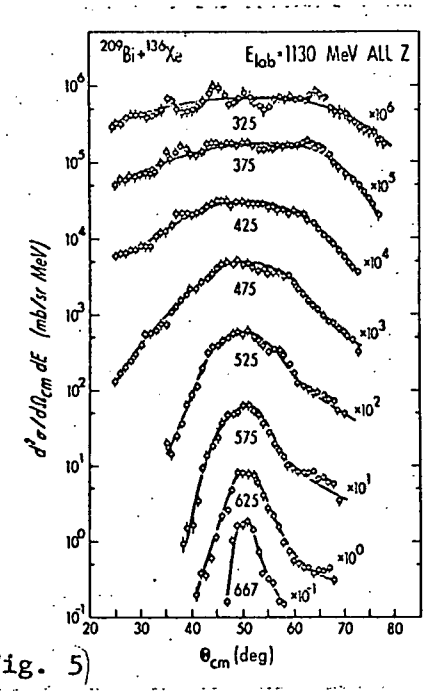

Fig. 5

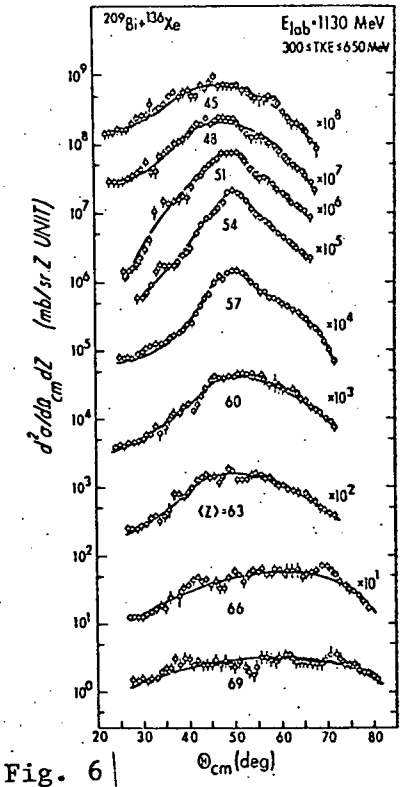

Fig. 6

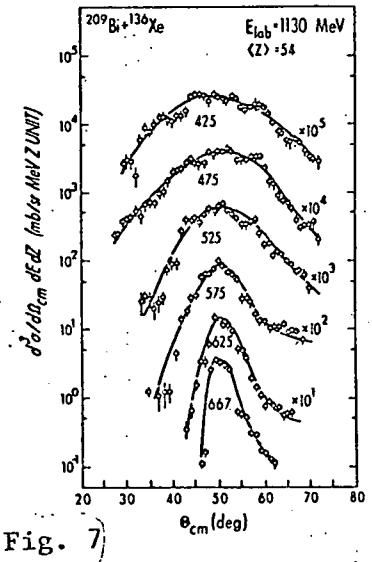

Fig. 7

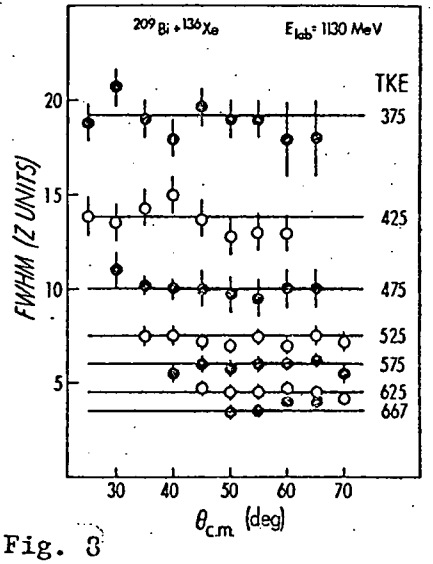

Fig. 8

B. Mass Exchange: Dependence on Energy Damping

There is by now considerable experimental evidence for an intimate correlation between the kinetic energy loss and the angular-momentum dependent interaction time. Hence, it is important to study mass correlations as a function of kinetic energy loss. An alternate parameter to the kinetic-energy loss is the dissipated kinetic energy. The two quantities are related by $E_{diss} = TKE_{loss} + [V_C(f) - V_C(i)]$ and are approximately the same when the differences between the Coulomb energies of the final and initial fragments are small.

The differential cross section $d^2\sigma/dZd(TKE)$ is plotted as a function of total kinetic energy (TKE) for different element bins in Fig. 9 for $^{209}Bi + ^{136}Xe$ reaction. Corrections for the emission of neutrons emitted during the de-excitation of the fragments have also been applied to the data. For Z values near the projectile the spectra contain sizable high-energy components and as Z decreases or increases, the spectra become softer. Hence, the degree of energy damping is a function of the mass of the product. For Z values near the projectile, the spectra contain events of a very wide range of kinetic energies, whereas large net Z transfers are correlated with high degrees of damping. Exit channel Coulomb energies for spherical fragments are indicated by the arrows. It is interesting to notice that (net) stripping and pickup both lead to roughly the same energy spectrum and cross section.

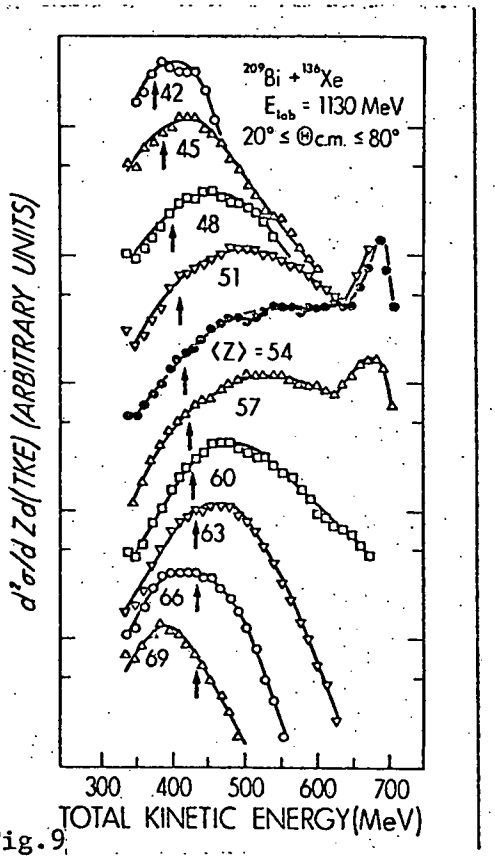

Fig. 9

One of the most informative ways to examine the relationship between the charge (or mass) distribution and the final kinetic energy is a plot of the differential cross section $d^2\sigma/dZd(TKE)$ as a function of Z for different final kinetic energy bins. Such a plot is shown in Fig. 10 where the energy bins are 50 MeV wide. The curves represent gaussian fits to the experimental data. It is readily seen that the width in the charge distribution increases markedly as the kinetic energy decreases. However, the centroid of the charge distribution stays constant at $Z \approx 55$ for a wide range of energy damping.

Such symmetric fragment Z distributions are very suggestive of a diffusive process evolving in time while kinetic energy is lost progressively.

A quantitative correlation between the measured variances of the charge distribution and the amount of kinetic energy loss is shown in Fig. 11 for four different heavy ion reactions.[3] Although the mass distributions are in general angle-dependent, in the case of Xe-induced reactions, the variance is independent of reaction angle for events of the same kinetic energy loss (see Fig. 8). The variance of the charge distribution increases smoothly with increasing total kinetic energy loss. However, the slope of the energy dissipation as a function of variance is largest for small variances and decreases as the variance increases.

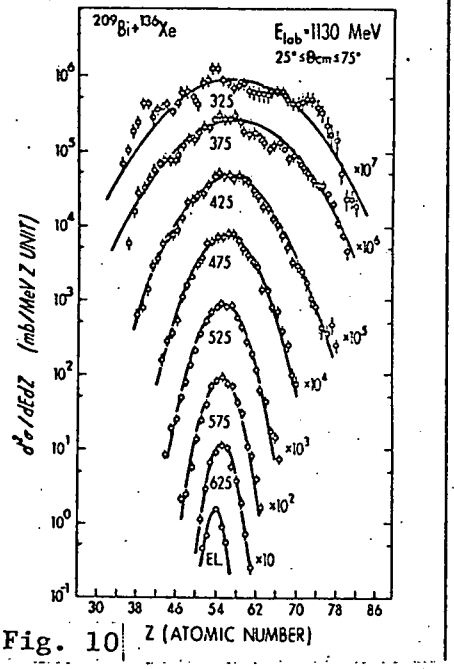

Fig. 10

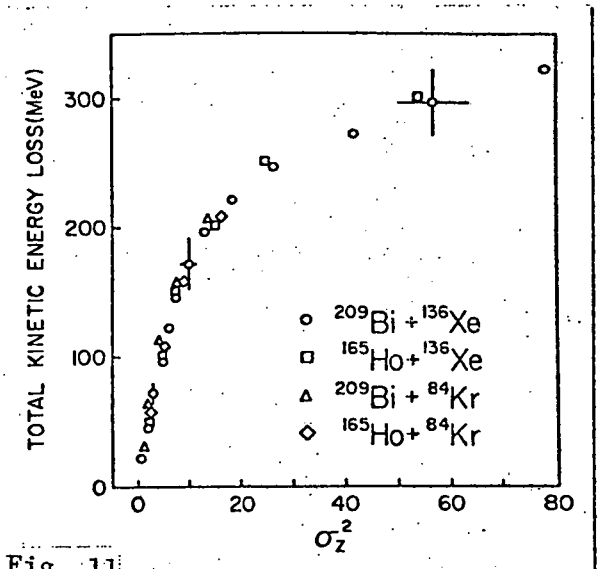

Fig. 11

The observed correlation between energy loss and the variance of the fragment Z distribution is of basic importance for understanding the damped reaction mechanism. Since many reaction channels are open, such reactions are clearly subject to statistical considerations. Regarding nucleon exchange in damped reactions as a random-walk process, the variance of the mass or Z distribution increases as a function of interaction time. Classical dynamical calculations[5,6] suggest that the interaction time increases with decreasing ℓ. The mean rate of nucleon exchange has also to increase with decreasing ℓ because the degree of matter overlap increases. Therefore, different ℓ waves corresponding to different interaction times will certainly lead to different values σ_Z^2 of the variance of the Z distribution. Hence, the σ_Z^2 axis on Fig. 11 represents a macroscopic time or ℓ scale for the damped heavy-ion collisions under consideration. It is conceivable

that in a nucleon exchange process kinetic energy does not always have to be lost but may also be gained, e.g., by decreasing the Coulomb energy. However, the important conclusion to be drawn from the experimental correlation displayed in Fig. 11 is that on the average kinetic energy is lost monotonically with decreasing ℓ and increasing interaction time, at least for a range of low and intermediate energy losses. This relation will be used in the following section to actually deduce the macroscopic time scale of damped heavy-ion reactions.

IV. INTERACTION TIMES OF DAMPED COLLISIONS

Little information is available on the interaction time scale on which heavy-ion collisions occur with various degrees of kinetic energy damping. A knowledge of these interaction times is essential for an understanding of the mass, kinetic energy loss and angular distributions of the reaction products from heavy-ion collisions. Strong focusing of the angular distribution for very heavy-ion reactions (see Fig. 1) suggests an angular-momentum dependence of the interaction time since many impact parameters lead to the same reaction angle.

Experimental evidence on fragment Z distributions, such as presented in the preceding section, suggests that during the time the two constituents of the intermediate double-nucleus system interact with each other, a mass equilibration process proceeds which is accompanied by a damping of the relative kinetic energy into other degrees-of-freedom. Since the equilibration processes are not completed during the short interaction times encountered in collisions between the very heavy ions under consideration, the amount of kinetic energy lost signifies the stage of evolution of the system and, hence, the total interaction time experienced. This view is supported by classical dynamical calculations[5,6] which show that the energy loss is a monotonic function of the initial angular momentum and the total interaction time. Associated with each interaction time is a Z distribution which is characterized by a variance σ_Z^2.

In the present analysis[7] we assume, following the discussion of Fig. 11 in the previous section, a monotonic increase in the total kinetic energy (TKE) loss with decreasing values of the impact parameter (see the first paragraph of IIIB). For simplicity we employ a sharp cutoff model where the cross section for angular momenta up to ℓ_j is given by $\sigma_j = \pi\lambda\!\!\!^{-2}(\ell_j+1)^2$. Using the experimental results on the heavy-ion reaction cross section as a function of TKE loss, $d\sigma/d(\text{TKE loss})$, the angular momentum is related to the TKE loss by

$$\ell_i = \{(\ell_j+1)^2 - \frac{\Delta\sigma_{ij}}{\pi\lambda\!\!\!^{-2}}\}^{1/2} - 1 \qquad (1)$$

where $\Delta\sigma_{ij} = \sigma_j - \sigma_i$ is the cross section in a TKE window $E_i \leq \text{TKE} \leq E_j$.

The procedure for converting energy loss to ℓ is illustrated in Fig. 12. Starting with ℓ_{max} and zero TKE loss, a deflection function is constructed from the experimental data, for a range of the higher ℓ values. Examples of such deflection functions are shown as solid lines in Figs. 13 and 14 for the $^{165}Ho + ^{84}Kr$ ($E_{Lab} = 714$ MeV) and $^{209}Bi + ^{136}Xe$ ($E_{Lab} = 1130$ MeV) reactions, respectively. The plotted angles represent the angles where the cross section is at a maximum for a particular kinetic energy loss. For the first reaction the emission angle of the lighter fragment decreases as ℓ decreases, whereas for the second reaction the emission angle is almost independent of ℓ. For each reaction the energy damping and the variance in the Z distribution both increase as ℓ decreases.

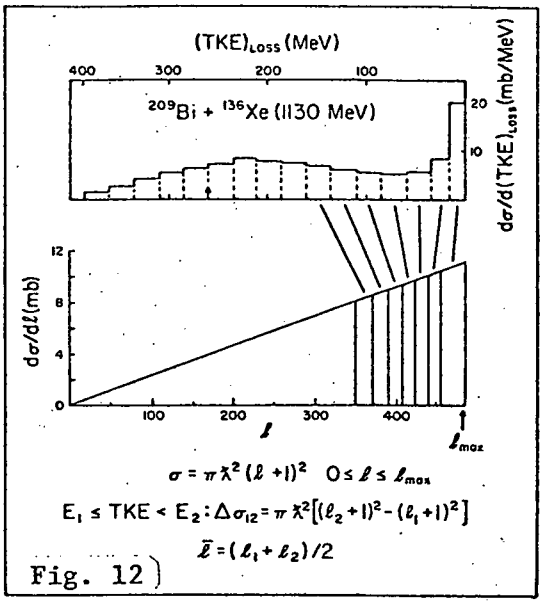

Fig. 12

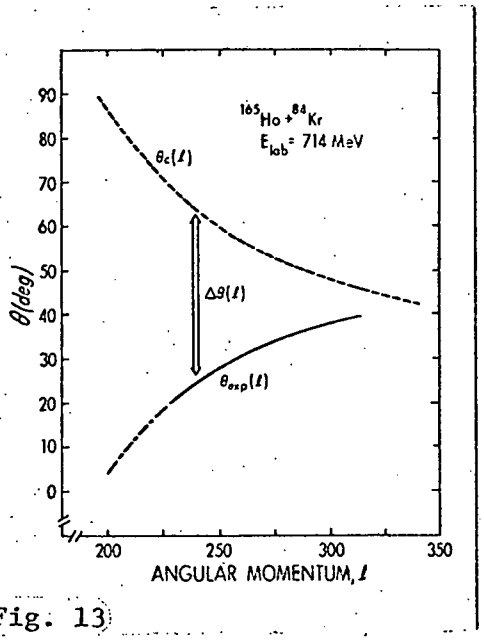

Fig. 13

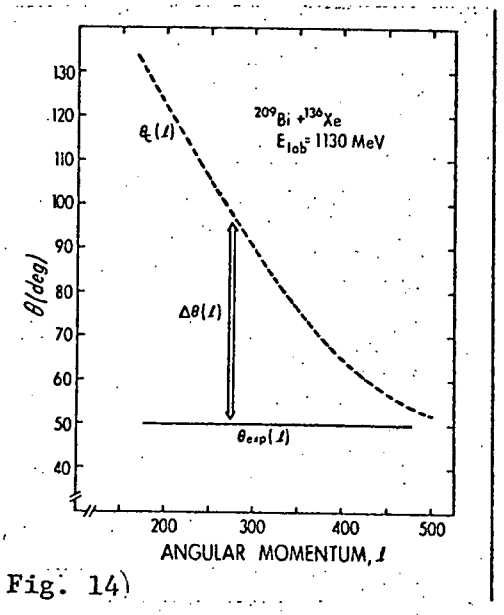

Fig. 14

The angular-momentum-dependent interaction time is calculated with the expression

$$\tau(\ell) = \Delta\theta(\ell)\, \mathcal{I}(\ell)/\hbar\ell \qquad (2)$$

where $\Delta\theta(\ell)$ is the difference between the Coulomb deflection angle $\theta_C(\ell)$ and the actual reaction angle $\theta_{exp}(\ell)$ and $\mathcal{I}(\ell)$ is the moment-of-inertia of the double-nucleus system. The Coulomb deflection angle

is estimated by

$$\theta_c(\ell) = 180^\circ - \theta_1 - \theta_3 \tag{3}$$

where the subscripts refer to the entrance and exit channels, respectively, and

$$\theta_j = +\arccos\frac{1}{\varepsilon_j} - \frac{K_j + R_j}{\varepsilon_j R_j} \quad (\text{for } j = 1 \text{ and } 3) \tag{4}$$

In Equation 4 the parameters ε and K are determined by

$$\varepsilon = \left[1 + \frac{2E\ell^2\hbar^2}{\mu(Z_pZ_Te^2)^2}\right]^{1/2} \tag{5}$$

$$K = \frac{\ell^2\hbar^2}{\mu Z_pZ_Te^2} \tag{6}$$

The above procedure for estimation of $\Delta\theta(\ell)$ is illustrated in Fig. 15. The evaluation of $\tau(\ell)$ requires the adoption of a collision model. Here we present the results of calculations with two rather different models which are labelled as "nonsticking" (NS) and "sticking" (S) collisions. A sticking collision is defined by rigid rotation of the double-nucleus system as a whole. By a NS collision we specify that the entrance and exit channel orbital angular momenta are the same ($\ell_f = \ell_i$) and the moment-of-inertia $\mathcal{I}_{NS} = \mu R^2$ where $\mu = M_1M_2/(M_1 + M_2)$ and R is the contact radius of the double-nucleus system (in the calculation the strong absorption radius R_{SA} is used). In contrast to a nonsticking collision, the final orbital angular momentum is inserted into Eq. 2 for a sticking collision, where $\ell_f = (\mathcal{I}_{NS}/\mathcal{I}_S)\ell_i$ and $\mathcal{I}_S = \mathcal{I}_{NS} + (2/5)(M_1R_1^2 + M_2R_2^2)$. The moment-of-inertia to be substituted into Eq. 2 is again $\mathcal{I}_{NS}$. In the calculations presented, any variation in $\mathcal{I}_{NS}$ with angular momentum or time is neglected. In Figs. 13 and 14, Coulomb deflection functions are shown for the "nonsticking" (NS) model.

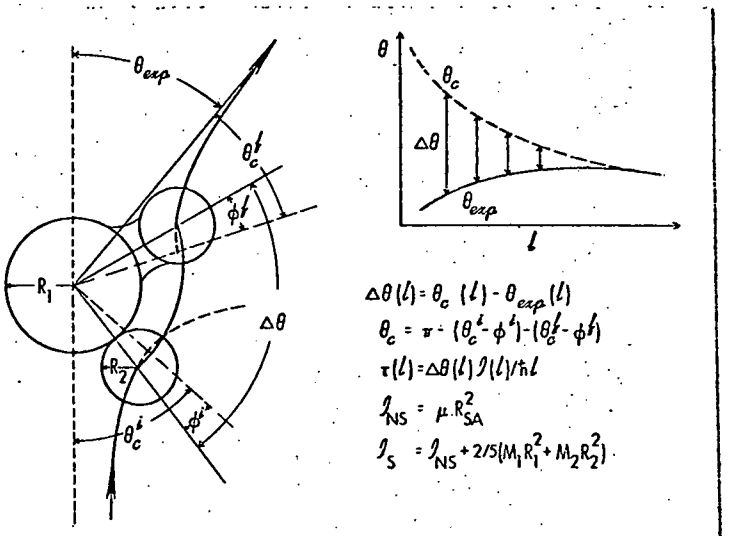

Fig. 15

The above definition of the deflection during the reaction implies that no kinetic-energy loss due to dissipation or dynamical deformation effects occurs at separation distances larger than the strong-absorption radius R_{SA}. The agreement of realistic deflection function calculations with experimental angular distributions for the heavy systems considered here suggests that the deviation of the trajectory with $\ell = \ell_{max}$ from a pure Coulomb trajectory is small. This indicates that all trajectories are similar to Coulomb orbits up to the strong-absorption radius. Hence, for $\ell < \ell_{max}$, the difference between Coulomb and observed deflection is used to evaluate the angle through which the intermediate system rotates during the nuclear interaction.

It should, however, be realized that it is, in principle, impossible to characterize the reaction between very heavy ions by a single deflection function. For such systems there are many intrinsic degrees-of-freedom coupled to the collective motion, and many different reaction paths may lead to similar values of a given experimental observable. Therefore, selecting a certain value of one experimental variable leads to a distribution of values of another variable fluctuating around its mean value. In this sense, the deflection functions derived above represent only average experimental deflection functions.

The angular-momentum-dependent interaction times calculated by the above procedure (see Eq. 2) are displayed in Fig. 16 for the nonsticking model. Multiplication of the angular momentum ℓ by the factor $[10^6(A_T+A_p)^{1/3}/(Z_T+Z_p)^2]\cdot(1/\ell_{max})$ produces straight lines on a semilog plot of approximately the same slope for the three reactions. The angular momentum range for the $^{209}Bi + ^{136}Xe$ reaction shown in Fig. 16 is $120 \leq \ell \leq 430$. For both the sticking and nonsticking models the interaction time is given empirically by the relation $\tau(\ell) = \tau_0 \exp(-\alpha\ell)$. Values of τ_0 and α for the three reactions shown in Fig. 16 are listed in Table 1.

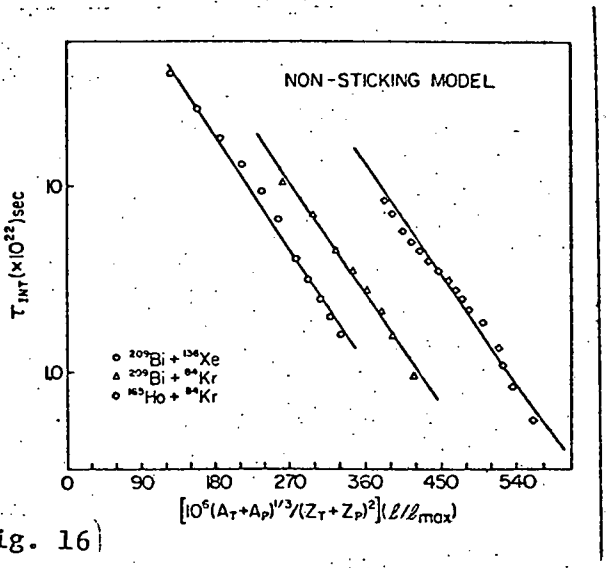

Fig. 16

TABLE 1

Functional parameters of the interaction times as deduced from a fit of the relation $\tau(\ell) = \tau_0 \exp(-\alpha\ell)$ to the data.

Reaction	E(lab)	Model	τ_0(sec)	α
$^{209}Bi + ^{136}Xe$	1130	S	1.86×10^{-20}	0.00974
		NS	2.18×10^{-20}	0.0118
$^{209}Bi + ^{84}Kr$	712	S	5.16×10^{-20}	0.0171
		NS	6.62×10^{-20}	0.0205
$^{165}Ho + ^{84}Kr$	714	S	1.65×10^{-19}	0.0224
		NS	1.62×10^{-19}	0.0244

V. NUCLEON DIFFUSION

The experimental charge distributions shown in Fig. 10 are suggestive of a diffusion process and have been analyzed with a Fokker-Planck equation in terms of the variance σ_Z^2. In its simplest form with one observable x and constant drift and diffusion coefficients, v and D, respectively, the Fokker-Planck equation has Gaussian solutions[8]

$$P(x,t) = (4\pi Dt)^{-1/2} \exp\{-(x-vt)^2/4\,Dt\} \tag{7}$$

The centroid $x_0 = vt$ and the variance $\sigma^2 = 2Dt$ are linear functions of the interaction time. The drift coefficient v_A is related to the diffusion coefficient through the Einstein relation,

$$v_A(A_1) = -\frac{1}{T} D_A \frac{\partial}{\partial A_1} U_\ell(A_1) \tag{8}$$

where U_ℓ denotes the ground-state energy of the combined system with relative angular momentum ℓ and fragmentation A_1. The local temperature T is determined by the excitation energy.

A relationship between experimental values of the total kinetic energy loss and the variance σ_Z^2 of the fragment charge distributions for very heavy damped collisions is shown in Fig. 11. This relationship in conjunction with the experimental cross sections as a function of the total kinetic energy loss is used to calculate angular-momentum-dependent values of the variance $\sigma_Z^2(\ell)$. In the above theory of nucleon diffusion, the value of $\sigma_Z^2(\ell)$ is related to the interaction time $\tau(\ell)$ by

$$\sigma_Z^2(\ell) = 2D_Z(\ell)\tau(\ell) \tag{9}$$

The interpretation of the experimental fragment Z distributions in terms of Eq. 9 is subject to similar observations as made above for the construction of an experimental deflection function. The experimental variance σ_Z^2 of the Z distribution is an average value determined by the range of ℓ waves contributing to a given TKE window. A factorization of σ_Z^2 according to Eq. 9 into mean values of D_Z and τ applies

only if $D_Z(\ell)$ is a slowly varying function of both Z and ℓ because the above analysis suggests that the total interaction time $\tau(\ell)$ is a rapidly varying function decreasing exponentially with increasing ℓ. This requirement on $D_Z(\ell)$ seems, indeed, to be fulfilled as indicated by model calculations and an experimentally observed small drift coefficient v_Z.

The value $\tau(\ell)$ entering Eq. 9 is the mean value of the time during which the nucleon diffusion mechanism operates. In this analysis it is assumed that $\tau(\ell)$ is the total interaction time evaluated by the procedure outlined above. However, it is conceivable that nucleon diffusion occurs only during a part of this time, although there is presently no experimental evidence for such a division of the total interaction time.

Values of $\tau(\ell)$ and $\sigma_Z^2(\ell)$ determined for the $^{165}Ho + ^{84}Kr$ (E_{Lab} = 714 MeV) and the $^{209}Bi + ^{136}Xe$ (E_{Lab} = 1130 MeV) reactions are plotted in Figs. 17 and 18, respectively.[7] The two different sets of values

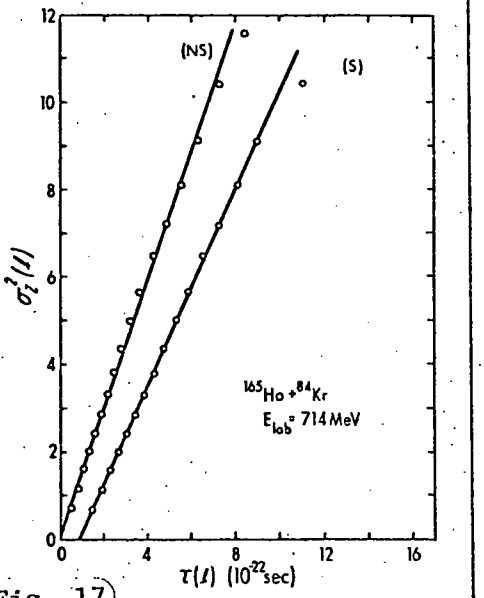

Fig. 17

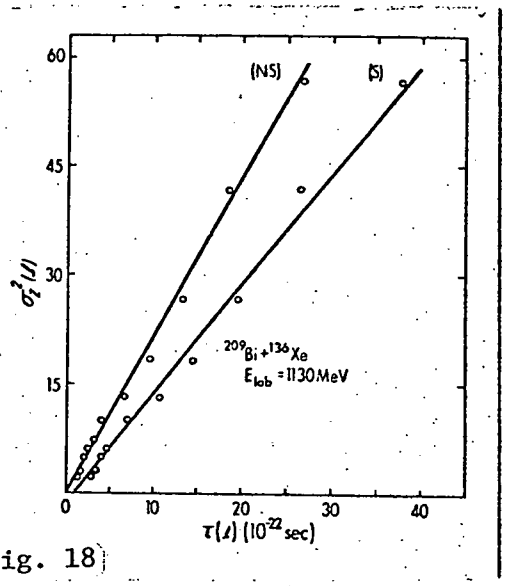

Fig. 18

of $\tau(\ell)$ for each reaction in this figure are based on the above NS and S models. The values of the diffusion coefficients for three heavy ion reactions determined by the slope of the line fitted to the $\sigma_Z^2(\ell)$ vs $\tau(\ell)$ data are given in Table 2 for each of the above two models. The proton number diffusion coefficient does not refer to proton diffusion alone, but to mass diffusion measured by the number of transferred protons. Assuming a conservation of the equilibrium Z/A ratio, the proton number (D_Z) and mass number (D_A) diffusion coefficients are related by $D_Z = (Z/A)^2 D_A$.

Table 2

Proton number (D_Z) and mass number (D_A) diffusion coefficients in units of 10^{22} sec^{-1} for Kr- and Xe-induced reactions.[7] The proton number diffusion coefficient does not refer to proton diffusion alone, but to mass diffusion measured by the number of transferred protons; hence, $D_Z = (Z/A)^2 D_A$ for a constant Z/A ratio. The diffusion coefficients listed in this table are calculated from the slopes of lines drawn through plots of $\sigma_Z^2(\ell)$ vs $\tau(\ell)$ over a range of ℓ values. In the case of the sticking model, for example, the points for the highest ℓ waves do not lie on a line which passes through the origin (see Figs. 17 and 18). Individual values of $D_Z(\ell)$ for the sticking model are ℓ dependent and increase initially as ℓ decreases. The Kr- and Xe-projectile energies (lab) are 714 and 1130 MeV, respectively. The errors in the diffusion coefficients are of the order of 30%. However, the values scale with the contact radius (see Eqs. 2 and 9) which for the reported values is assumed to be the strong absorption radius, R_{SA}.

Reaction	Sticking Model		Nonsticking Model	
	D_Z	D_A	D_Z	D_A
$^{209}Bi + ^{136}Xe$	0.75	4.8	1.1	7.0
$^{209}Bi + ^{84}Kr$	0.62	3.7	0.87	5.3
$^{165}Ho + ^{84}Kr$	0.55	3.2	0.74	4.3

V. MECHANISMS OF KINETIC ENERGY DISSIPATION

In previous sections evidence has been presented to show that kinetic energy loss and mass exchange are strongly correlated. This result is consistent with the view that nucleon diffusion evolves in a continuous fashion as energy is dissipated and supports a close correspondence of the time scales governing energy dissipation and nucleon exchange. In this section we employ the microscopic time scale provided by the nucleon exchange process to study the energy dissipation mechanism.

At the heavy-ion bombarding energies discussed here and moderate excitation energies, one expects that nucleon exchange and particle-hole excitation without nucleon exchange are mediated by the one-body interaction given by the single particle field. Such a mechanism gives rise to classical friction forces proportional to the relative velocity v of the two ions,[10-12]

$$\vec{F} = -k\vec{v} \tag{10}$$

In general, k is an anisotropic tensor dependent on the separation distance of the two ions, which is equivalent to an implicit time dependence of k. The importance of one-body friction in nuclear fission and heavy-ion reactions has been discussed also by other

authors.[13-17] Two-body friction induced by inelastic scattering of individual nucleons of target and projectile, which may also play a role in energy dissipation, has in general a velocity dependence more complicated[18] than that implied by Eq. 10.

The energy loss rate associated with Eq. 10 is

$$-dE/dt = 2(k/\mu)E \tag{11}$$

where μ is the reduced mass. Integration of Eq. 11 with a constant coefficient k gives

$$\ell n(E_0/E) = 2(k/\mu)t \tag{12}$$

where $E_0 = E_{c.m.} - E_B$, $E = E_0 - E_{loss}$ and $E_{c.m.}$ and E_B are the incident c.m. kinetic and Coulomb energies, respectively. Employing the microscopic time scale provided by the nucleon exchange process, namely

$$d\sigma_Z^2/dt = 2D_Z(t) \tag{13}$$

and substituting this relation into Eq. 11 and integrating leads to a relation

$$\ell n(E_0/E) = (k/\mu D_Z)\sigma_Z^2 \tag{14}$$

provided that the ratio (k/D_Z) is independent of time. Hence, a linear relation is predicted between $\ell n(E_0/E)$ and σ_Z^2. Such a plot is shown in Fig. 19 where E_B is calculated at the strong absorption radius. Good agreement between experiment and this simple theory is obtained for energy losses up to 200 MeV. If k/D_Z is the same for Kr- and Xe-induced reactions at a bombarding energy of 8.5 MeV/amu, the slopes of Fig. 19 lead to

$$k/D_Z = (0.9 \pm 0.3) \times 10^{-43} \text{ MeV sec}^2 \text{ fm}^{-2}. \tag{15}$$

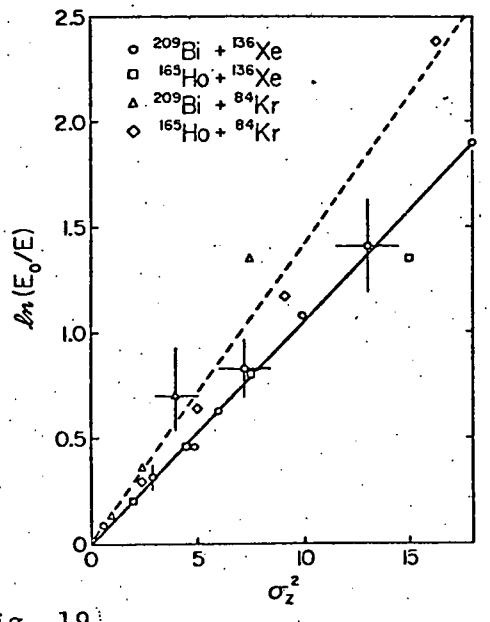

Fig. 19

The result of a constant friction coefficient rather than a strongly varying form factor as suggested by classical dynamical calculations[11,12,19] can be understood as being due to the fact that in the analysis reference was made to a nucleon diffusion mechanism in order to derive a microscopic time scale.[3] Although it is presently not quite clear to what extent the one-body dissipation mechanism applies, the experimental results are consistent with the view that energy dissipation mediated by nucleon exchange and the other possible dissipation mechanisms proceed on a similar microscopic time scale and have a similar

dependence on the separation distance of the two ions and the angular momentum. In principle, a fast dissipation mechanism[20] operating only during a small initial part of the total interaction time cannot be excluded. However, it has to lead to a friction-like relation between the energy loss and the total interaction time which is similar to Eq. 11 in order to fit the data.

An interesting new experimental observation[21,22] is that k/D_Z increases as the bombarding energy decreases. For example, as the bombarding energy is reduced from 1130 to 970 MeV for the $^{209}Bi + ^{136}Xe$ reaction, the value of k/D_Z increases[21] by a factor of more than 2.

Kinetic energy is known to be lost in nucleon exchange between target and projectile.[23] In a simple version of a one-body nucleon exchange process[13], where a nucleon of mass m is assumed to be loosely bound and at rest with respect to the donor nucleus, its relative momentum $\Delta p = mv$ is dissipated in the transfer. The resulting loss of total kinetic energy per nucleon exchange δE_{ex} is then proportional to the kinetic energy available prior to exchange[24],

$$\delta E_{ex} = (m/\mu)(E_{c.m.} - E_B - E_{loss}) = (m/\mu)E \qquad (16)$$

where $\delta E_{ex} = (-dE_{ex}/dt)/(dN/dt)$ and dN is the number of exchanged nucleons per unit time dt. Consequently, the energy loss rate for nucleon exchange alone is

$$-dE_{ex}/dt = (m/\mu)E(dN/dt) = k_{ex}v^2 \qquad (17)$$

This energy loss rate is equivalent to that due a friction force $F_{ex} = -k_{ex}v$ (see Eq. 10) with a frictional coefficient,

$$k_{ex} = (m/2)(dN/dt) \qquad (18)$$

where $(dN/dt) = 2(A/Z)D_Z$. The total number N of nucleon exchanges is obtained from the number $N_Z = \sigma_Z^2$ of protons exchanged by scaling N_Z according to the mass-to-charge ratio, $N = (A/Z)\sigma_Z^2$. This is justified by the experimental observation of a fast equilibration[1] of the mass-to-charge asymmetry degree-of-freedom in damped heavy-ion reactions which indicates that neutron and proton exchange rates are similar. Substitution of dN/dt into Eq. 18 gives

$$(k_{ex}/D_Z) = m\,(A/Z) \qquad (19)$$

where m is the nucleon mass. Converting the units of erg sec^2 cm^{-2} to MeV sec^2 fm^{-2}

$$(k_{ex}/D_Z) = 0.1044 \times 10^{-43}\,(A/Z)\ \text{MeV sec}^2\,\text{fm}^{-2} \qquad (20)$$

For the $^{209}Bi + ^{136}Xe$ reaction at a bombarding energy of 1130 MeV, it follows that k_{ex}/D_Z is approximately 30% of k/D_Z (see Eq. 15). Hence, energy dissipation caused directly by the nucleon exchange process

represents only a fraction of the total energy dissipation. Furthermore, this fraction decreases as the bombarding energy is reduced.

If one denotes the friction force coefficient due to one-body dissipation processes such as particle-hole excitation without nucleon exchange by k_{nex}, the resulting total energy dissipation rate (in analogy to Eq. 11) is

$$-dE/dt = (2/\mu)(k_{nex} + k_{ex})\, E \qquad (21)$$

It may be expected that the rates of one-body processes without and with nucleon exchange represented by the friction coefficients k_{nex} and k_{ex}, respectively, are somewhat different in magnitude. However, since both processes are induced by the same time-dependent single-particle potential, the two friction coefficients are expected to have the same time dependence. This is equivalent to both friction forces having the same spatial form factor. Under this condition, the energy loss rates due to particle-hole excitation and nucleon exchange are proportional to each other. The microscopic time scale corresponding to the nucleon exchange mechanism may then be used to calculate the total energy loss during the time necessary for one-nucleon exchange. Consequently, this <u>total</u> energy loss associated with a single exchanged nucleon, δE, is given by

$$\delta E = -d(E_{nex} + E_{ex})/dN = (m/\mu)[1 + (k_{nex}/k_{ex})]E \qquad (22)$$

Similar arguments apply to the case of two-body friction and exchange which, in general, give rise to a more complicated energy dependence.[18]

Experimental results for the energy loss per nucleon exchanged for the reactions[3] $^{165}Ho + ^{84}Kr$, $^{165}Ho + ^{136}Xe$ and $^{209}Bi + ^{136}Xe$ at a bombarding energy of 8.5 MeV/amu and for the reaction[25] $^{197}Au + ^{86}Kr$ at 7.2 MeV/amu are presented in Fig. 20. The values of δE were obtained by differentiating curves of E_{loss} vs N fitted to the experimental data points. The estimated errors are, therefore, correlated. The $^{197}Au + ^{84}Kr$ data were transformed into the center-of-mass system assuming ^{84}Kr-kinematics for all fragments.

The most important observation to be made from the data is that the energy δE dissipated during the time necessary for the exchange of a single nucleon decreases with decreasing available kinetic energy E (i.e. increasing energy loss and total excitation energy of the system). The

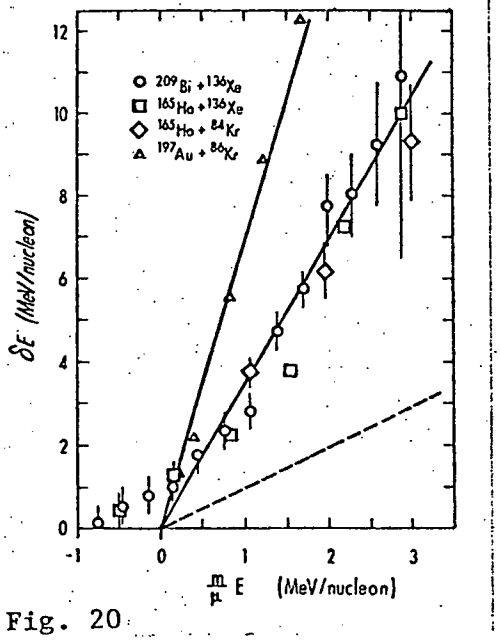

Fig. 20

data points follow a straight line intercepting the abscissa at $(m/\mu)\,E = 0$ as predicted by Eq. 22 over an unexpectedly wide range of available energies. For small available energies the data points deviate from these lines. This indicates that large energy losses may lead to a highly deformed intermediate system. Hence, the Coulomb energy may be much lower than the one in the entrance channel, which is used to calculate the available energy. On the other hand, the one-body mechanism may also lose importance at high excitation energies, where the Pauli principle is less inhibitive for two-body nucleon collisions.

As is indicated by the dashed line in Fig. 20 corresponding to Eq. 16 (or to Eq. 22 with $k_{nex} = 0$), energy dissipation by nucleon exchange alone can account for ~30% of the total energy loss for the 8.5 MeV/amu data and for ~15% for those at 7.2 MeV/amu. The good description of the data by the linear relation predicted by the one-body mechanism suggests that the ratio k_{nex}/k_{ex} is, indeed, constant over a wide range of excitation energies and ℓ values. Although the $^{197}Au + ^{86}Kr$ data[26] exhibit a linear dependence on the available energy, they do not lie on the line determined by the 8.5 MeV/amu reaction data. Studies[21,22] of similar reactions at various bombarding energies indicate that nucleon exchange accounts for a smaller fraction of the total energy loss as the bombarding energy is reduced.

The diffusion model proposed by Nörenberg and collaborators[26-28] treats nucleon exchange and energy loss on the same basis accounting for the dependence of the transport coefficients on excitation energy or energy loss. Noticing that the rates of energy loss and nucleon exchange are determined by the energy drift coefficient v_E and the mass diffusion coefficient D_A according to $dE/dt = -v_E$ and $dN/dt = (2Z/A)D_A$, one obtains[28]

$$\delta E = \frac{A}{Z}\frac{v_E}{2D_A} = \frac{A}{Z}\frac{\Delta^2}{8}\frac{(g_1+g_2)^{1/2}}{(g_1 g_2)^{1/3}}\,(g_1^{1/3}+g_2^{1/3})^2\,E_{loss}^{-1/2} \qquad (23)$$

for the total energy dissipated during the exchange of one nucleon. Here, $\Delta \approx 2.5$ MeV is a mean value of the energy dissipated in one nucleon exchange or particle-hole excitation process, and $g_k = A_k/12$ are the single-particle level density parameters of the two ions.

Theoretical curves represented by Eq. 23 are compared in Fig. 21 with the experimental energy loss per nucleon as a function of energy loss. The level density parameters were calculated for the projectile-target combination of fragments. As can be seen in Fig. 21, the diffusion model can account for the high energy loss observed per nucleon exchange for low values of kinetic energy loss corresponding to small interaction times.[2] However, the predicted functional dependence (Eq. 23) is not supported by the data. It is interesting to notice that on this plot also the $^{197}Au + ^{86}Kr$ data follow the experimental systematics for small values of E_{loss}. If the diffusion model is modified to account for the reaction dynamics employing

5. D.H.E. Gross, H. Kalinowski and J.N. De, Symposium on Classical and Quantum Mechanical Aspects of Heavy Ion Collisions, Heidelberg, 1974, Springer Verlag, Lecture Notes in Physics 33(1975)194.

6. K. Siwek-Wilczyńska and J. Wilczyński, Nucl. Phys. A264(1976)115.

7. W.U. Schröder, J.R. Birkelund, J.R. Huizenga, K.L. Wolf and V.E. Viola, Jr., Phys. Rev. C16(1977) August issue.

8. W. Nörenberg, Phys. Letts. 52B(1975)289.

9. S. Ayik, B. Schürmann and W. Nörenberg, Z. Physik A279(1976)145.

10. R. Beck and D.H.E. Gross, Phys. Lett. 47B(1973)143.

11. D.H.E. Gross and H. Kalinowski, Phys. Lett. 48B(1974)302.

12. D.H.E. Gross, Nucl. Phys. A240(1975)472.

13. W.J. Swiatecki, Lawrence Berkeley Laboratory Report LBL-4296 (1975); Jour. Phys. C5(1972)45 and private communication.

14. J. Blocki, Y. Boneh, J.R. Nix, J. Randrup, M. Robel, A.J. Sierk and W.J. Swiatecki, Annals of Physics (1977) in press.

15. J. Randrup, preprint 1977.

16. S.E. Koonin, R.L. Hatch and J. Randrup, to be published in Nucl. Phys.

17. S.E. Koonin and J. Randrup, preprint 1977.

18. K. Albrecht and W. Stocker, Nucl. Phys. A278(1977)95.

19. D.H. Gross and H. Kalinowski, 4. Session d'Études Biennale de Physique Nucléaire, La Toussuire, France, 1977.

20. R.A. Broglia, C.H. Dasso and Aa. Winther, Phys. Lett. 61B(1976) 113.

21. W.W. Wilcke, J.R. Birkelund, W.U. Schröder, J.R. Huizenga, A. Mignerey, D.G. Raich, K.L. Wolf and V.E. Viola, to be published.

22. A. Mignerey, D.G. Raich, R.L. Boudrie, K.L. Wolf, V.E. Viola, J.R. Birkelund, W.U. Schroder and J.R. Huizenga, to be published.

23. P.J. Siemens, J.P. Bondorf, D.H.E. Gross and F. Dickmann, Phys. Lett. 36B(1971)24.

24. W.U. Schröder, J.R. Huizenga, J.R. Birkelund, K.L. Wolf and V.E. Viola, Jr., preprint (1977).

25. L.G. Moretto and J.S. Sventek, Proceedings of the Symposium on Macroscopic Features of Heavy-Ion Collisions, Argonne, 1976, Regport ANL/PHY-76-2, p. 235.

26. W. Nörenberg, Z. Physik A274(1975)841.

27. S. Ayik, B. Schürmann and W. Nörenberg, Z. Physik A277(1976)299.

28. S. Ayik, B. Schürmann and W. Nörenberg, Z. Physik A279(1976)145.

velocity-proportional friction forces, the result is quite similar to one-body dissipation.

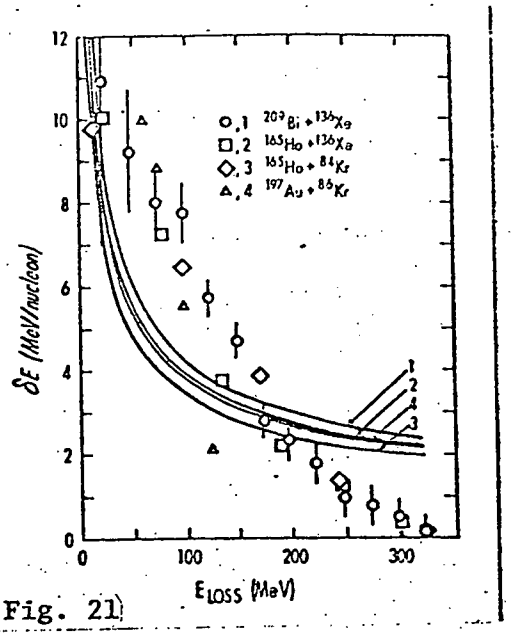

Fig. 21

In conclusion, the observed correlation between nucleon exchange and energy loss suggests that the microscopic time scale provided by the exchange mechanism can be used to study the energy dissipation mechanism in heavy-ion reactions. The experimental energy loss associated with a single nucleon exchange exhibits a linear dependence on the available kinetic energy, as predicted by a one-body dissipation mechanism. The diffusion model can account for high amounts of energy dissipated per nucleon, δE, for low energy losses; however, it does not predict correctly the decrease of δE with increasing energy loss. Neither model accounts directly for the increase of k_{nex}/k_{ex} (or k/D_Z) with decreasing bombarding energy.

Acknowledgments

†The authors acknowledge the contributions of V.E. Viola, Jr. and K.L. Wolf to the results reported in this paper.

*Work supported by the U.S. Energy Research and Development Administration.

**Supported in part by a grant from the German Academic Exchange Service DAAD

***Supported by a grant from the National Science Foundation

References

1. W.U. Schröder and J.R. Huizenga, Ann. Rev. Nucl. Science 27(1977). References to the literature of damped heavy ion reactions can be found in this review article and, hence, only a limited number of references to results discussed here are included.

2. W.U. Schröder, J.R. Birkelund, J.R. Huizenga, K.L. Wolf, J.P. Unik and V.E. Viola, to be published.

3. J.R. Huizenga, J.R. Birkelund, W.U. Schröder, K.L. Wolf and V.E. Viola, Jr., Phys. Rev. Letts. 37(1976)885.

4. J. Wilzcyński, Phys. Lett. B47(1973)484.